A 2D full-waveform inversion using trench-deployed surface and VSP DAS data from CaMI FRS

Luping Qu*, Wenyong Pan, Kris Innanen
luping.qu1@ucalgary.ca

Abstract

Based on the previous surface-wave full-waveform inversion (FWI). A full-waveform inversion using trench-deployed surface waves and two wells' Vertical Seismic Profiling (VSP) data was conducted to generate a high-resolution S- and P-wave velocity models of the near surface at Containment and Monitoring Institute Field Research Station in Alberta. In this preliminary inversion, a sequential inversion was conducted by firstly inverting Vs using surface-wave FWI, and secondly inverting Vp using the VSP FWI. There are two datasets collected in August 2022 for the main CO_2 monitoring line, line 13. They possess the same frequency range, with linear and low-dwell sweep, respectively. In this study, we compared these two datasets in detail. The inversion results are from the DAS data generated using the low-dwell sweep. Optical transport method was adopted to mitigate the cycle skipping problem mainly in surface wave inversion.

Introduction

By utilizing all of the wave modes present in the data, full waveform inversion (FWI) of surface wave data tries to recover the elastic properties of the near-surface. However, in FWI, when the initial model is not close to the true model, cycle skipping due to the non-convexity of FWI problem can happen, which is related to the oscillatory nature of seismic data. The cycle skipping issue is amplified by the surface wave's dispersive nature and its shorter wavelengths. Alternative misfit functions have been suggested as a solution (Borisov et al., 2018). An alternative method to mitigate cycle skipping is optical transport (OT). The idea is to take advantage of the inherent convexity of optimal transport distances with respect to translation and dilation. Engquist and Froese firstly introduced the idea of using optimal transport for seismic inversion (2014).

DAS is a novel technology for seismic acquisition that measures phase changes of back-scattered laser pulses (Rayleigh scattering) induced by transient vibrations incident on optical fiber. The phase changes are proportional to axial strain changes along finite segments of the fiber, referred to as *gauge length*. Therefore, strain rate (or strain) changes along the fiber are recorded. Compared to standard geophones, DAS has a series of advantages including dense spatial sampling, low-cost, easy installation, etc.

In August, 2022, more datasets were collected from the field data tests. Over 100 shots were collected from the line 13 using both linear sweep VP and low-dwell sweep VP, with the frequency range of 2-150 Hz. 10 shots with high Signal-to-Noise Ratio (SNR) were selected from these data. The location of the field and geometry for these 10 shots are shown in Figure 1.

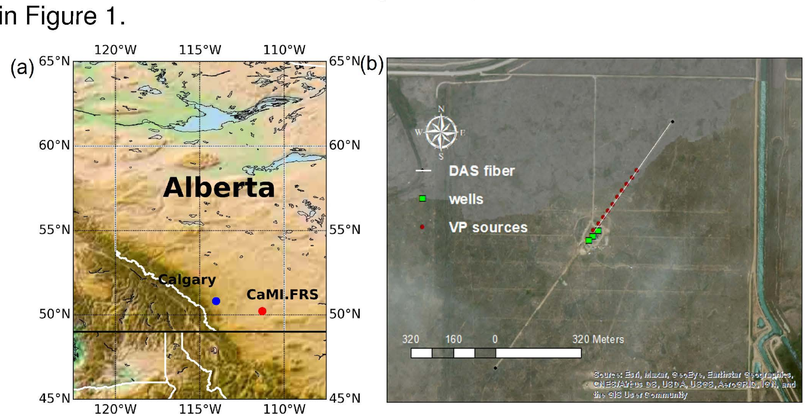

Figure 1: The location of CaMI FRS and geometry for the dataset.

Methods

In a typical FWI formulation, model parameters are iteratively updated by minimizing the direct waveform-difference (WD) between the synthetic data u_i and observed seismic data d_i, which can be formulated as a L-2 norm misfit, e.g.,

$$\Phi(\mathbf{m}) = \frac{1}{2}\sum_{r=1}^{N_r}\int_0^{t'}\int_V \left[u_i(\mathbf{x}_r, t; \mathbf{m}) - d_i(\mathbf{x}_r, t)\right]^2 d\mathbf{x}dt, \quad (1)$$

where $\mathbf{m}$ is the model vector, $\mathbf{x}_r$ indicates the rth receiver location with a maximum number of N_r, t' is the maximum recording time and V denotes the whole volume containing all subsurface positions $\mathbf{x}$. Optimal Transport (OT)-based misfits can be interesting for FWI as they exhibit a wider convexity with respect to time shifts citep. Various formulations of OT applied to FWI exist, and all are related to Wasserstein distances. The p-Wasserstein distance for two PDFs $\rho_1(\boldsymbol{s}, \boldsymbol{r}, t)$ and $\rho_2(\boldsymbol{s}, \boldsymbol{r}, t)$ is

$$J^p_{W_p}(\rho_1, \rho_2) = \min_T \int d\boldsymbol{e} c_p^p(\boldsymbol{e}, \boldsymbol{E}_{\rho_1\rho_2}(\boldsymbol{e}))\,\rho_2(\boldsymbol{e}) \quad (2)$$

subject to the constraint $\boldsymbol{E}_{d_1 d_2} \in \boldsymbol{T}$ the set of maps on $\boldsymbol{e}$ that rearrange ρ_2 to ρ_1. e denotes a data coordinate space vector and c_p denotes the Lp distance between vectors in the data coordinate space. Equations above seek at the minimum cost to transport mass from ρ_2 to ρ_1 from the c_p^p point of view.

Results

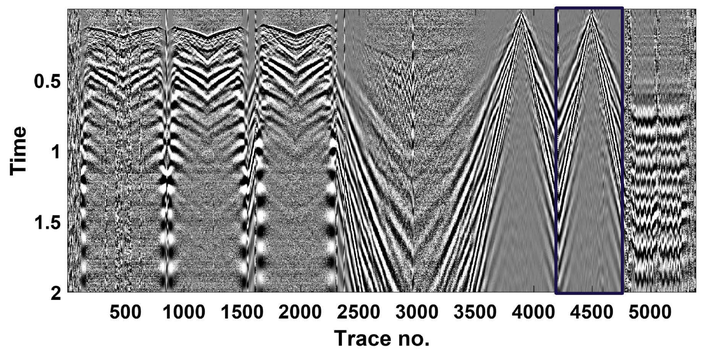

Figure 2: The dataset collected from line 13 using low dwell sweep VP (The framed part is the data used in this study).

After preprocessing including data conversion, filtering, denoising, a sequential FWI processing was conducted on the DAS straight-fiber data. At first, we conducted surface-wave full waveform inversion using the fundamental-mode Rayleigh waves with optimal transport method.The initial model and inverted Vs model is shown in Figure 3 and Figure 4.

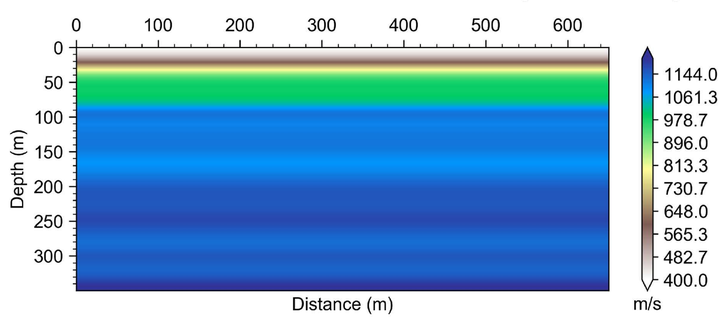

Figure 3: The initial model for surface-wave FWI.

Results

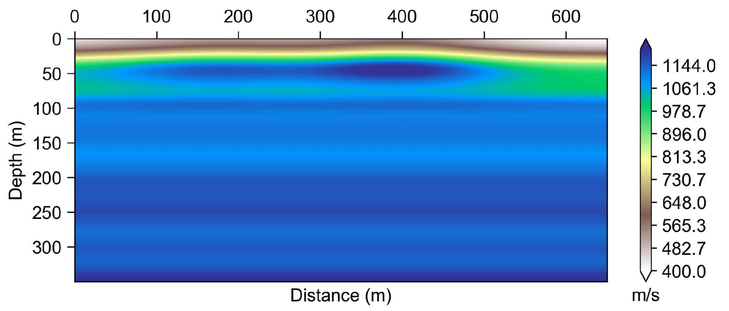

Figure 4: The inverted Vs model of surface-wave FWI.

Based on the obtained the Vs model, a VSP FWI was conducted using the DAS data collected from the straight fiber in the two wells. The inverted Vp model is shown in Figure 5.

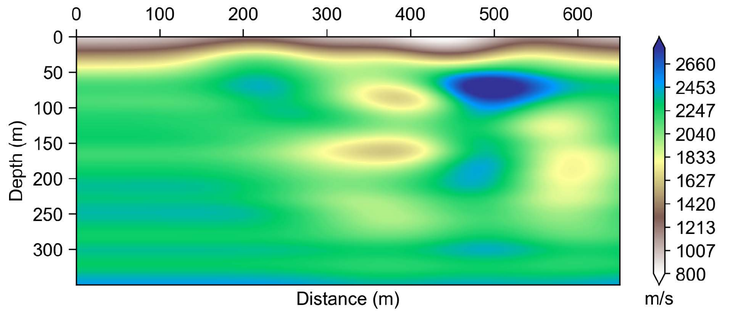

Figure 5: The inverted Vp model of VSP FWI.

O shown in the x-axis represents the NE end point of the DAS trench fiber. These are the preliminary inversion results of the surface-wave FWI and VSP FWI.

Conclusions

For surface-deployed straight fiber, only single-component high-amplitude surface wave data are collected. Thus, a rough Vs profile with limited depth can be obtained through the surface-wave FWI. However, engineering and researchers are more interested in the Vp profile in most cases. The straight-fiber DAS data collected from the wells can help invert the Vp profile with a high resolution. In this study, we adopted a sequential inversion strategy to firstly invert the Vs using surface-wave FWI with optical transport. Secondly, we conducted VSP FWI using the DAS datasets from the two wells to invert Vp based on the Vs profile obtained from the first round FWI.

References

- Engquist B, Froese B D. Application of the Wasserstein metric to seismic signals[J]. arXiv preprint arXiv:1311.4581, 2013.
- Métivier L, Brossier R, Mérigot Q, et al. Increasing the robustness and applicability of full-waveform inversion: An optimal transport distance strategy[J]. The Leading Edge, 2016, 35(12): 1060-1067.
- Borisov D, Modrak R, Gao F, et al. 3D elastic full-waveform inversion of surface waves in the presence of irregular topography using an envelope-based misfit function3D elastic FWI using envelopes[J]. Geophysics, 2018, 83(1): R1-R11.

NSERC CRSNG
UNIVERSITY OF CALGARY
FACULTY OF SCIENCE
Department of Geoscience
Carbon Management Canada